Low Temperature Physics ARTICLE scitation.org/journal/ltp

Nonlinear transport properties of atomic copper point contacts

Cite as: Fiz. Nizk. Temp. **49**, 908–915 (July 2023); doi: 10.1063/10.0019693
Submitted: 29 May 2023

Marcel Strohmeier, Kim Kirchberger, and Elke Scheer[a)]

AFFILIATIONS

Universität Konstanz, Fachbereich Physik, 78457 Konstanz, Germany

[a)]**Author to whom correspondence should be addressed:** elke.scheer@uni-konstanz.de

ABSTRACT

We report studies on the nonlinear electronic transport properties of copper point contacts. Utilizing the mechanically controllable break junction technique, various contact sizes can be realized to study ensemble-averaged differential conductance spectra at low temperatures. We investigate signatures of phonon excitations for contact sizes down to the atomic scale, where conductance fluctuations arise superimposing the phonon signatures. Applying high bias voltages to atomic-size copper contacts reveal additional features caused by atomic rearrangements.

1. INTRODUCTION

The history of point-contact spectroscopy (PCS) started in the 1970s pioneered by I. Yanson[1–3] and coworkers. Their seminal studies on small metallic constrictions are considered path-breaking as they introduced novel concepts of spectroscopy by measuring not only the conductance of a system but also its derivatives. In mesoscopic conductors, this can reveal signatures of fundamental excitations and electronic interactions.[4] Meanwhile, after a few decades of ongoing progress in nanofabrication, PCS has been widely established as a powerful tool in solid-state physics, but it had even impact on related fields like molecular electronics.[5] Thereby, the metallic structures under study became continuously smaller, necessary to experimentally access transport regimes close to the (quasi-)ballistic limit. A powerful approach to explore quantum transport properties in low dimensions is given by the mechanically controllable break junction (MCBJ) technique.[6,7] Here, clean point contacts of various sizes down to single-atom contacts can be realized with very high precision. In contrast to other approaches based on scanning tunneling microscopes (STM) or electromigration setups, break junctions offer both an appropriate stability, but also reversibility and tunability when it comes to the formation of ultrasmall nanostructures.[5] Obviously, this will be helpful when transport properties are studied from a statistical point of view.

Regarding quantum point contacts comprehensive research on a variety of different materials, such as (semi-) metals, ferromagnets or superconductors, has been carried out.[8] Especially the three noble metals gold, silver and copper have always gained a special attention,[8–11] mainly because of their relatively simple electronic configuration in combination with relatively low chemical reactivity. Since the electronic transmission function of single-atom contacts of these metals is dominated by a single channel arising from the highest *s*-orbital, they serve as an ideal test bed system to explore the basic concepts of quantum transport.[12]

For atomic-scale copper (Cu) contacts predominantly the conductance histogram has been studied in the literature[10,13,14] to gain deeper insights into the origin of conductance quantization. It is known that Cu typically exhibits two prominent conductance peaks, one around 1 G_0 linked to the single-atom contact and another one slightly below 3 G_0, where the contact reveals approximately three transmitting modes.[10] In general, this observation confirms the three-dimensional electron gas character of the metallic constriction.[15,16] A third peak with a significantly lower amplitude can be localized between 1.5 and 2 G_0 and has been attributed to another stable atomic configuration.[10,13] It was also shown that cold metal working will affect the physical properties of Cu nanowires, in particular, the conductance and the visibility of its discreteness.[14]

Spectroscopic measurements on Cu have been carried out by Jansen and coworkers[17–19] mainly on large contacts with a typical junction resistance of a few Ω. Their experimental findings verify phonon excitations at around 17 and 28 mV for the transversal-acoustic (TA) and longitudinal-acoustic (LA) mode, respectively. This is in a good agreement with calculations based on

the Eliashberg spectral function,[20] but also with the phonon density of states obtained from neutron scattering experiments.[21] Interestingly, the recorded point-contact spectra demonstrate that the first peak associated with the TA modes is significantly stronger than the second LA feature. A similar trend can be observed on Au and Ag point contacts,[17] and, therefore, it has been assumed that for noble metals in general the coupling between transverse phonon and the electron gas is much more efficient.[22] A possible explanation is given in the work of Lee *et al.*[20] that considers normal and Umklapp transitions within the framework of large-angle scattering. It suggests that the energy and polarization dependence triggers the partial suppression of LA modes.

2. EXPERIMENTAL SECTION

2.1. Sample preparation

We investigate atomic Cu point contacts by MCBJ at low temperature in a dipstick immersed in a bath cryostat, which provides also cryogenic vacuum conditions. The samples are fabricated on phosphor bronze substrates coated with a sacrificial layer of polyimide. The nanopatterning is done by the well-established liftoff process.[5,23] Here, a two-layer resist consisting of a copolymer MMA-MAA and polymer PMMA is structured by electron-beam lithography, followed by electron beam evaporation of Cu. We choose a metal film thickness of 80 nm. After liftoff, all samples pass a final step of O_2 plasma etching to form a free-standing metallic constriction with a typical width of around 100 nm (cf. Fig. 1).

2.2. Electronic transport measurements

To determine the contact resistance, we apply a four-point measurement scheme. To this end, a bias voltage is applied, and the direct current (dc) as well as the voltage drop across the break junction are probed. Additionally, we measure the differential conductance dI/dV with the conventional lock-in-technique by simply adding a small sinusoidal alternating current (ac) amplitude to the signal. The modulation amplitude used in our measurements is typically in the order of 1 mV. Each dI/dV measurement on a stable point-contact configuration is performed symmetrically by sweeping the voltage source from negative to positive polarity (cf. Fig 2). An initial sweep towards the starting point preserves the sample from abrupt voltages drops and, therefore, enhances the contact stability.

3. RESULTS

To avoid any contamination, a MCBJ is cooled down in its unbroken state. Only under cryogenic vacuum conditions a three-point bending mechanism stretches the sample to gradually thin out the constriction and to finally break it apart to form a tunnel contact. Next, a sequence of conductance vs. distance curves is recorded, and a conductance histogram is computed out of the opening traces. From such a statistical analysis, one can estimate the cleanliness of the contact, but it also gives valuable information about the breaking behavior and stability of single-atom contacts. A typical conductance histogram, which was recorded on one of the two samples with an applied bias voltage of 10 mV, is shown in

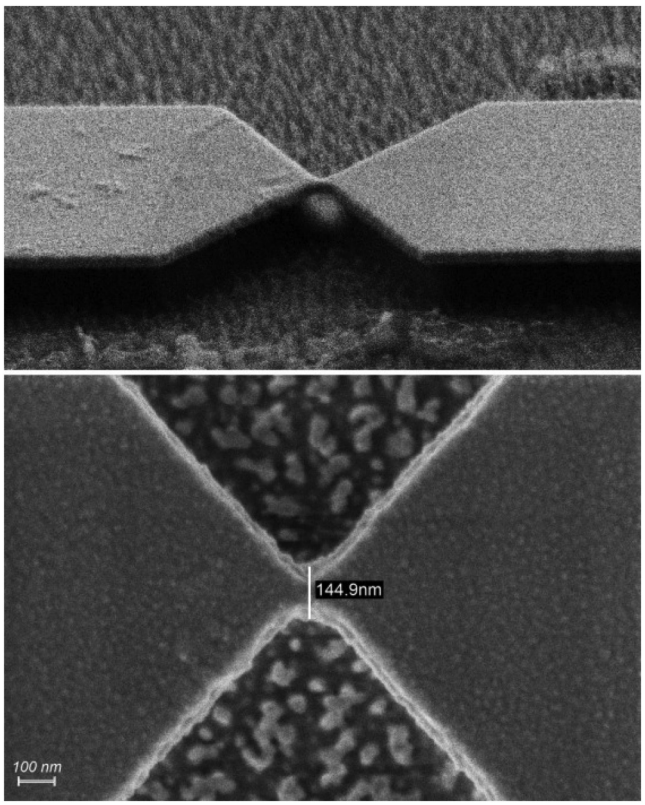

FIG. 1. Scanning electron micrographs of a Cu break junction. Top: Freestanding metallic constriction connected to the leads in a side view. Bottom: Zoom onto the constriction in top view.

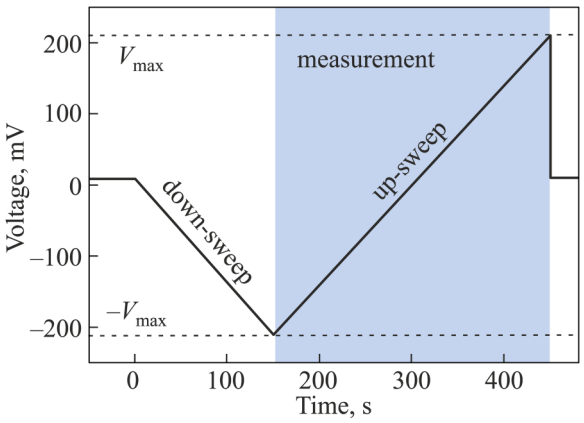

FIG. 2. Measurement scheme for recording the differential conductance of atomic contacts. After an initial ramp to $-V_{max}$ (down-sweep), the voltage is swept to $+V_{max}$ (up-sweep). If an instantaneous conductance jump occurs during the up-sweep, a contact is sorted out and not considered in the data evaluation.

Fig. 3. In accordance with previous studies,[10,14] it features two prominent peaks at around 1 and 2.65 G_0 with lower peak height for the higher conductance value. In between, we can identify a less pronounced indication of another preferred atomic configuration, which is localized slightly below 2 G_0. Also this structure is known from the literature, although it has been found that this intermediate peak is sensitive to details of the experiment.

3.1. Point-contact spectroscopy

In order to study nonlinearities in the current-voltage characteristics, we first performed PCS measurements on a Cu nanobridge. Thereby, a rather low bias voltage up to 40 mV is applied, where even atomic-size contacts are usually proven to be stable.[24] During the whole voltage sweep, the differential conductance dI/dV across the sample is recorded. If any inelastic electron interactions, such as phonon excitations, are present, they will affect the electron transport and, therefore, the total current measured at a certain excitation energy. Hence, to recognize small nonlinearities, it is a common practice to analyze the first derivative of the differential conductance. Within this approach, inelastic scattering events are then associated with point symmetric features in the numerically calculated d^2I/dV^2 spectrum. In the present work, we primarily focused on the ensemble-averaged differential conductance, for which a larger amount of different point contacts has been subsequently measured.

Between each measurement, the break junction was completely broken and sufficiently closed to ensure that each time a new atomic configuration is formed. Nevertheless, we assume that an ensemble averaging requires a set of contacts with similar junction resistances. Any feature and trend in the dI/dV that survives an average over several contact configurations, can then provide information about generic transport properties of Cu atomic contacts.

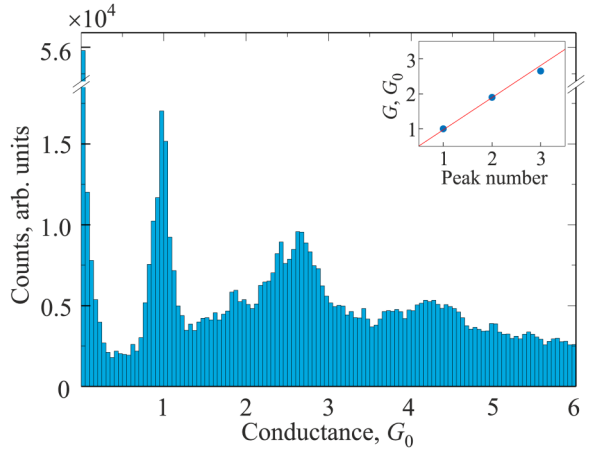

FIG. 3. Conductance histogram obtained from 279 consecutively recorded opening traces recorded at 4 K.

Apart from that statistical approach, MCBJs were used to realize variable contact sizes. This involves single-atom contacts, as well as larger contacts with a conductance up to 50 G_0. To identify any type of size effects, our PCS spectra have been grouped into four point-contact regimes with average conductance of 1 G_0 (54 contacts), 10 G_0 (86 contacts), 30 G_0 (111 contacts), and 50 G_0 (55 contacts), respectively. In practice, however, the junction conductance, which refers to the zero bias value, can vary by 10% within one ensemble. As shown in Fig. 4, each set of measurement is illustrated by a color-coded two-dimensional (2D) histogram. Using this representation helps to highlight distinctive features in the $(d^2I/dV^2)/(dI/dV)$ versus voltage, where an additional normalization has been applied. It is evident that the PCS spectra of the largest contacts follow a nearly point symmetric trend with a pronounced negative peak (dip) at around ±18 mV. We attribute this feature to phonon excitations, as it matches the TA energy reported in the literature.[17–19] It is remarkable that the appearance of the ensemble averaged peaks is in general rather broad and shows a V-shaped character. Additional features towards higher voltages are not visible in the spectra. This might be in accordance with previous observations[17–20] on even larger Cu point contacts of a few Ω, where excitations of LA modes have been shown to be less pronounced. Taking into account the differences in the junction resistance, it seems that LA-related signals are totally suppressed by reducing the dimensions further.

To give a qualitative interpretation, we recall that the PCS spectrum d^2I/dV^2 is directly proportional to the electron-phonon interaction (EPI) spectral function $g(\omega) = \alpha^2F(\omega)$, where $F(\omega)$ is the phonon density of states and α^2 being the square of the EPI matrix element.[4] From Cu, it is expected that the distortion of the Fermi surface, which approaches the boundary of the Brillouin zone, will enable Umklapp transitions by involving transverse phonons.[1,20] For point-contact geometries, this is mainly caused by large-angle scattering processes. The dominance of the TA peak relative to its LA counterpart was also explained theoretically by showing that the polarization factor in the electron-phonon matrix enhances the first TA peak tremendously considering the polarization and spectral distribution of the available phonon states.[20] As of the Umklapp scattering, the contribution of longitudinal phonons is strongly suppressed, and also the scattering angles for normal transitions are physically limited to the belly of the Cu Fermi surface,[20] Hence, the finding that $\alpha^2_{LA} \ll \alpha^2_{TA}$ leads to the conclusion that Umklapp processes caused by the interaction of electrons with transverse phonons are dominant throughout the whole energy spectrum.[1] Therefore, it seems plausible to measure a strongly TA dominated PCS spectrum. The fact that LA-related features are totally suppressed might be a consequence of changes in the DOS and Fermi surface in atomic-size contacts where the electronic structure can differ from the bulk properties. Another possible explanation involves the electron mean free path, as it has been shown that the LA peak intensity correlates with the cleanliness of the sample.[4,25] However, this seems unlikely, as we follow a statistical analysis on a sample which is made of high purity Cu (99.999%) and broken only under cryogenic conditions.

Furthermore, we can point out that the overall peak height decreases as we move to smaller contact sizes down to the atomic scale. In the 2D histogram, which summarizes the 10 G_0

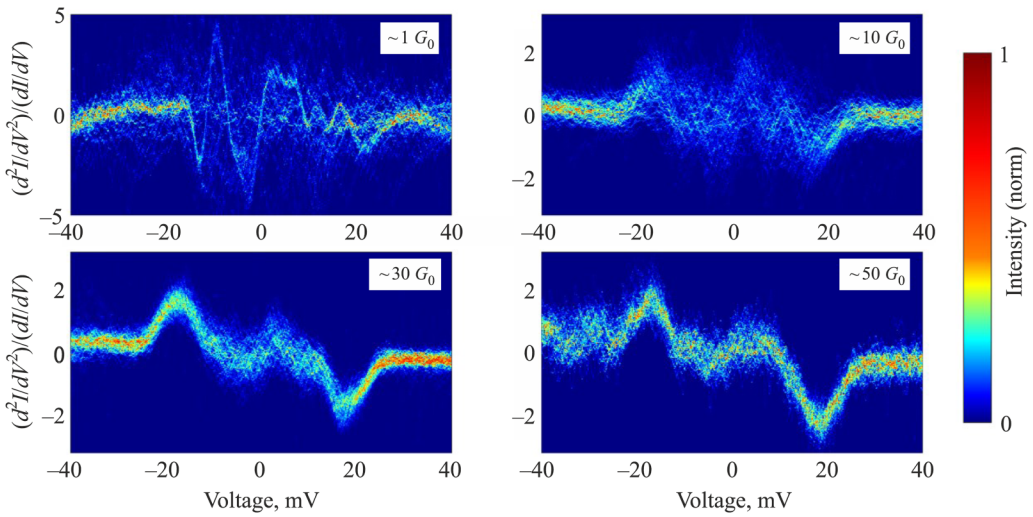

FIG. 4. Point-contact spectroscopy: 2D histograms of the normalized derivative of the differential conductance $(d^2I/dV^2)/(dI/dV)$ for ensembles of contacts with similar junction conductance. The measurements has been grouped into four point-contact regimes with a conductance of around 1, 10, 30, and 50 G_0, respectively. The averaged PCS spectra of large contacts clearly follow a point symmetric trend with a pronounced peak around 18 mV, which can be attributed to phonon excitations. With decreasing contact size, the peak amplitude seems to shrink as a consequence of the reduced effective scattering volume probed by the voltage sweep. Simultaneously, at the atomic-scale, conductance fluctuations arise in the signal where they superimpose the weak phonon signatures.

measurements, only faint traces of the phonon signatures are still visible. We attribute this size effect to the reduced effective scattering volume around the point contact. Since the PCS spectrum is predominantly sensitive to electron-phonon interactions in the direct vicinity of the constriction,[5] the dimensions will indeed affect the measured signal across the junction. For atomic-sized contacts, there are only a few atoms left forming the contact. Hence, instead of probing the bulk phonons, we rather excite vibrational modes of atomically localized configurations. On this scale of mesoscopic transport, also conductance fluctuations become increasingly important. Therefore, in the limit of single-atom contacts (Fig. 4, top-left histogram), one can assume that fluctuations superimpose the weak phonon signals. This applies, in particular, for an ensemble of atomic contacts with different channel configurations.[10]

To obtain more information from the first data set, we calculate the averaged $(d^2I/dV^2)/(dI/dV)$ spectrum composed of 54 individual measurements. In addition, a symmetry operation $f(V) = [f(V) - f(-V)]/2$ is applied to suppress non-point-symmetric spectral features. The resulting PCS spectrum in Fig. 5 shows indeed a curvature, which resembles the phonon feature observed for larger contacts. Both the excitation energy as well as the trend in the signal amplitude are in line with the other results in Fig. 4. It is worth mentioning that the symmetrized spectrum shows some kind of subfeature with two separate dips localized at around 16 and 24 mV. However, it remains an open question whether this (averaged) signal reflects two different vibration modes, or is simply the result of noise. As discussed above, LA modes of Cu are expected to appear at 28 mV, at least for larger contacts treated in the literature.[17–19]

3.2. Conductance at high voltages

In general, quantum coherent transport through atomic contacts is described as an electron wave-scattering process. Hence, within the well-known Landauer formalism, conductance is a property, which measures the sum of the transmission probabilities of individual transport channels. It is important to note that although the concept of finite transmissions refers directly to the electrons, it does not only give access to purely electronic variables. Also other

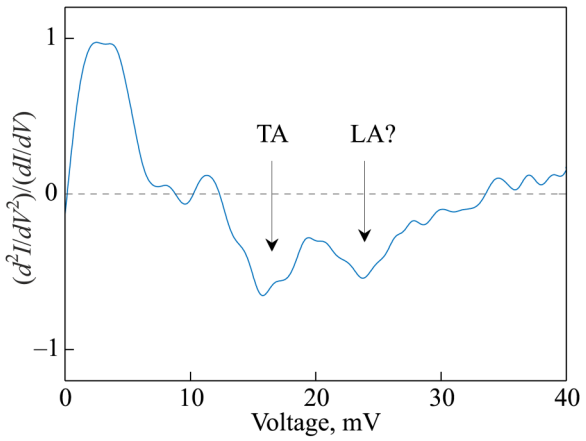

FIG. 5. Ensemble-averaged and symmetrized PCS spectrum composed of *dI/dV* measurements on 54 atomic-size contacts with a conductance around 1 G_0.

phenomena such as spin-dependent transport, thermal transport or even the thermopower are connected with it. Therefore, studying the conductance gives insight into electronic properties, but in fact it even allows to correlate different measurable quantities.

Here, we are especially interested in the high-voltage dependency of the dI/dV. Applying high bias voltages to atomic contacts is known to be limited, as at a certain threshold V_{th} voltage-induced rearrangements are triggered. This was experimentally studied on break junctions of different materials,[26] together with complementary theoretical simulations showing strong evidence for a phonon-mediated origin.[24] For the present study on atomic Cu junctions, we still perform voltage sweeps, as schematically shown in Fig. 2. During the whole cycle, the dI/dV is recorded, even though for the statistical analysis only the full sweep from $-V_{max}$ to V_{max} (up-sweep) is used. V_{max} is settled between 200 and 320 mV, which turned out to be a good compromise to produce a sufficiently large statistics. As can be seen from Fig. 6, choosing the right interval is indeed a trade-off, since conductance jumps start to arise even at lower voltages. The depicted example also shows that whenever a jump in the dI/dV was detected, we apply a symmetric cut to the data set, where the cut-off voltage $|\pm V_{cut}|$ lies below the threshold $|V_{th}|$. This step of data processing is necessary to ensure that each dI/dV characteristic is basically the fingerprint of one stable atomic configuration. In the following, all contacts are grouped according to their zero-bias conductance $G(V \approx 0)$.

As in the case of PCS, we still follow a statistical approach by studying a large number of atomic Cu contacts. A selection of the high-voltage measurements which passed the data processing is presented in Fig. 7. Here, the normalized differential conductance $(dI/dV)/(dI/dV\ (V=0))$ is shown as an ensemble-average up to a bias-voltage of 300 mV. The contacts are grouped into three regimes, namely 0.9–1.1 G_0, 1.8–2.1 G_0 and 2.5–2.8 G_0, chosen by the distinctive peaks in the conductance histogram. All three curves have in common that the mean value shows a negative trend towards a lower conductance when high voltages are applied. For the positive polarity, this trend seems to be more pronounced, but also more uniform among the different contact sizes. We note that at 300 mV the averaged differential conductance is decreased by roughly 5 to 10% depending on the selected conductance regime.

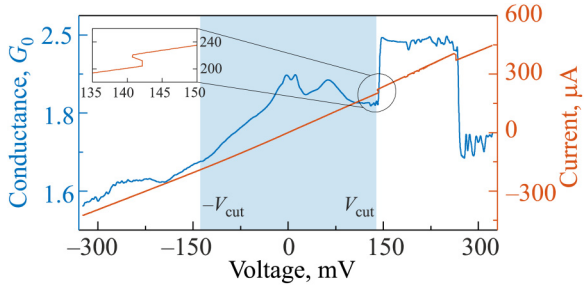

FIG. 6. An example of a dI/dV measurement, where a conductance jump occurred as a consequence of voltage induced atomic rearrangements. A symmetric cut is applied to the data set to ensure that only stable sweep intervals (shaded) are considered in the statistical investigations below.

For negative polarities, the overall slope of the averaged dI/dV appears almost linear, although more fluctuations are present. The appearance of an overall asymmetry with respect to the applied voltage is indeed remarkable, as we consider the mean differential conductance over a large amount of contacts. Hence, any ensemble average presented here is expected to reveal generic properties of a symmetric Cu-Cu contact configuration where accidental asymmetries are negligible, provided that the changes of the contact geometry performed by the mechanics involve all parts of the sample that are relevant for the symmetry. Hence, one possible explanation for the remaining asymmetry is that asymmetries on the mesoscale (~10–100 nm), which are outside the active manipulation range, are at the origin of the asymmetry. These might be caused by the in-built asymmetry in the measurement procedure arising from the voltage sweep direction itself. These considerations suggest that mesoscale electromigration might be responsible for the observed asymmetry. In addition, one can observe enhanced size effects where the negative bending of the ensemble average curve correlates with the contact size. Thereby, the dI/dV characteristic composed of single-atom contacts (0.9–1.1 G_0) seems to be the most remarkable one, because it hardly follows a symmetric trend. Also it exhibits a significant kink at around −200 mV, which appears much stronger than the other artifacts arising from different cut-off voltages. In order to understand this observation in

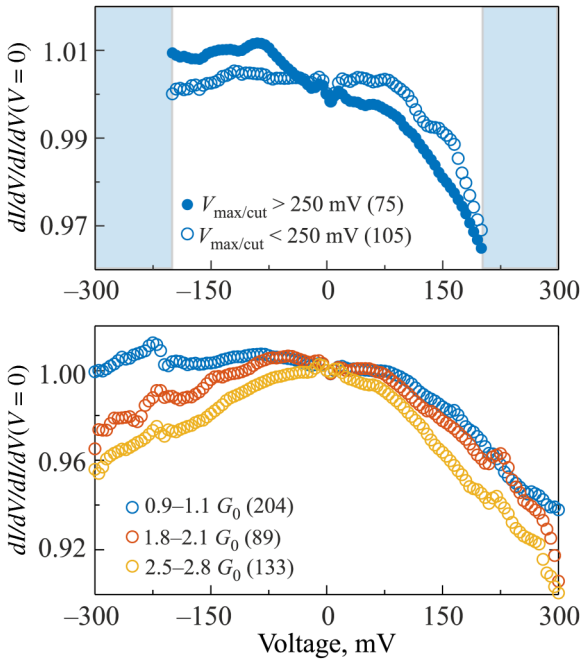

FIG. 7. Ensemble-averaged and normalized dI/dV versus voltage measurements on atomic Cu contacts. The mean trend is shown for different conductance intervals based on the three distinctive maxima in the conductance histogram. In the top panel, the data set for 0.9–1.1 G_0 is subdivided to illustrate the impact of the starting voltage on the dI/dV of single-atom contacts. The number of contacts is indicated in parentheses.

more detail, we further subdivide our set of single-atom contacts into two fractions and assign them depending on whether the voltages $|V_{max}|$ and $|V_{cut}|$ are above or below 250 mV. As depicted in the upper panel of Fig. 7, this results in two significantly different curves. On average, it turns out that contacts which have seen higher bias voltages are characterized by a stronger dI/dV asymmetry with respect to the voltage. That variation explains why for the entire data set a sudden jump appears between 200 and 225 mV. It is this range in which the cut-off voltage is settled for most of the contacts considered in the open-symbol data set. For the sake of clarity, the plotting is limited up to ±200 mV, since outside this range the discrete distribution of V_{cut} gives rise to additional small artifacts.

At this point, we can only speculate about reasons that might explain the discrepancy between the two curves in the upper panel of Fig. 7. It seems that in the case of atomic-size contacts the applied voltage $-V_{max}$ has an influence on the subsequent recording of the dI/dV. Such kind of memory effect in the conductance could be indeed the result of atomic rearrangements induced by the applied bias voltage. However, it remains a small effect, which has been only observed in the averaged and normalized dI/dV of around 100 single-atom contacts. Further studies are necessary to obtain more reliable information about this effect. Heating as an possible explanation seems unlikely as the subgroup of contacts with $V_{max/cut}$ >250 mV reveals a higher conductance. Furthermore, this effect is less pronounced for contacts with higher conductance (cf. Fig. 7), although one would expect the opposite trend, namely, more heating due to higher currents. In general, the observation of a rather monotonous negative trend in the differential conductance points towards heating that has to be taken into account.[4] As has been studied in detail, larger point contacts in the so-called thermal regime show a quadratic decrease of the conductance that can be translated into an enhanced local temperature.[4] Although the observation of the phonon peaks at smaller bias shows that the contacts studied here belong well to the ballistic regime, at such high bias a multitude of vibration modes will be excited and may lead to current-induced atomic rearrangements where gradual displacements of the central atoms can change the overall transmission.[24,27] This would be to some extent comparable to an elastic stretching of the contact, as it has been studied by differential conductance measurements on atomic gold wires.[28] However, we can point out that a similar statistical analysis carried out on the recorded base temperature in the immediate vicinity of the sample holder does not show any significant correlations which would point towards an increase in the measurement temperature.

The whole set of normalized dI/dV measurements on atomic contacts with a conductance between 0.6 and 6 G_0 is summarized in Fig. 8. In the 2D histogram, a similar trend towards lower conductance shows up when high voltages are applied to the MCBJ. From the data set that has been considered here, we derive a rather broad distribution of the maximum voltage that an atomic-size Cu contact can sustain. A statistical overview is given by the corresponding histogram in Fig. 8, where either $|V_{max}|$ or $|V_{cut}|$ is considered for a dI/dV that is entirely or partially stable, respectively. As mentioned in the previous paragraph, there is an accumulation of counts between 200 and 225 mV arising from the predefined choice of V_{max}. Apart from that, however, the histogram seems to

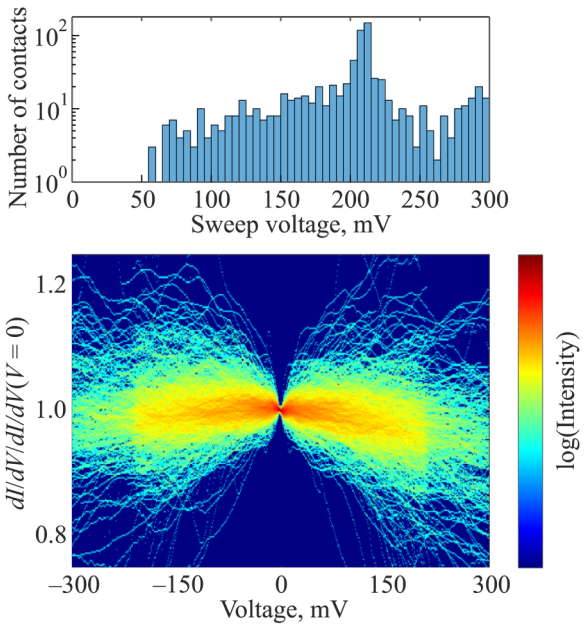

FIG. 8. 2D histogram summarizing 971 normalized dI/dV measurements on atomic-size Cu contacts with a conductance between 0.6 and 6 G_0. The color-coding reveals an overall negative trend of the conductance towards high bias voltages. The histogram illustrates the distribution of the maximum sweep voltage up to which an individual measurement has been detected as stable.

be fairly evenly distributed down to ~70 mV. This observation is consistent with the work of Ring *et al.*,[24] where the switching voltage of atomic Cu contacts was extensively studied.

4. CONCLUSION

In conclusion, we presented a comprehensive study on the elastic and inelastic electronic transport behavior of atomic-size contacts at low temperature. Cu was the material of choice in the early studies of point-contact spectroscopy, pioneered by I. Yanson, investigating nanometer-size contacts. It has attracted much less attention regarding atomic-size contacts compared to its nobel metal sister element Au, presumably because of its somewhat higher chemical reactivity. Nevertheless, as testbed system for more complex transport properties such as thermopower or shot noise, Cu might be preferable because it is a lighter element, the electronic properties of which are closer to the free-electron model and less contributions from spin-orbit coupling can be expected. Our studies show that lithographically fabricated Cu MCBJs show clean metallic properties that are consistent with earlier findings in the nm-size range. In the present study, we focus on small contacts and find that the properties of atomic-size contacts are again in agreement with existing studies using MCBJs from glued and notched wires.[13,29,30] By virtue of the high stability of thin-film MCBJs, we can also study individual contacts in detail and follow the behavior of phonon-induced nonlinearities as a function of contact size. Thereby, we rely on a statistical approach to obtain PCS spectra

which are constructed by ensembles of comparable point contacts. From the analysis, it becomes evident that, on average, phonon excitations are present in all configurations under study, from 50 G_0 contacts down to single-atom contacts. However, only one excitation signature was found at 18 mV, matching the TA energy reported in the literature.[17–19] We assume that, on the atomic scale, LA-related signals are tremendously suppressed, following a trend which was already observed on larger Cu contacts.[17–20] The observed correlation between the conductance and the height of the phonon peak can be interpreted as a size effect arising from the reduced effective scattering volume, as well as from conductance fluctuations on the atomic scale. Finally, the differential conductance measurements under high bias voltages reveal additional nonlinearities caused, most likely, by atomic rearrangements. From the ensemble-averaged and normalized dI/dV of atomic Cu contacts, we deduce an overall decreasing trend for increasing absolute bias voltage. Our statistical approach shows further voltage-induced asymmetries in the dI/dV characteristics of single-atom contacts, where atomic rearrangements might play a crucial role. Further studies with a stronger focus on the applied bias window and role of the sweep direction are necessary to address the role of mesoscale electromigration in more detail.

ACKNOWLEDGMENTS

We gratefully acknowledge fruitful discussion with R. Hoffmann-Vogel, P. Nielaba, F. Pauly, and M. Ring. We thank S. Haus for his assistance in sample preparation, as well as J. Maier and R. Sieber for their technical supports and supplying us with liquid helium. We further appreciate the preliminary work carried out by F. Herbst and R. Zerfaß, as well as P. Haiber, who initiated the studies on atomic Cu contacts in our group.

REFERENCES

[1]I. K. Yanson, Sov. Phys. JETP **39**, 506 (1974).
[2]I. K. Yanson, and Y. N. Shalov, Sov. Phys. JETP **44**, 148 (1976).
[3]I. K. Yanson, Sov. Phys. JETP **37**, 338 (1973).
[4]Y. G. Naidyuk and I. K. Yanson, *Point-Contact Spectroscopy* (Springer Series, New York, 2005).
[5]J. Cuevas and E. Scheer, *Molecular Electronics An Introduction to Theory and Experiment*, Nano Series, Vol. 15 (World Scientific Publishing, Singapore, 2017).
[6]C. J. Muller, J. M. van Ruitenbeek, and L. J. de Jongh, Physica C Supercond. **191**, 485 (1992).
[7]C. J. Muller, J. M. van Ruitenbeek, and L. J. de Jongh, Phys. Rev. Lett. **69**, 140 (1992).
[8]N. Agraft, A. L. Yeyati, and J. M. van Ruitenbeek, Phys. Rep. **377**, 81 (2003).
[9]J. M. Krans, C. J. Muller, I. K. Yanson, T. C. M. Govaert, R. Hesper, and J. M. van Ruitenbeek, Phys. Rev. B **48**, 14721 (1993).
[10]B. Ludoph, and J. M. van Ruitenbeek, Phys. Rev. B **61**, 2273 (2000).
[11]C. J. Muller, J. M. Krans, T. N. Todorov, and M. A. Reed, Phys. Rev. B **53**, 1022 (1996).
[12]E. Scheer, N. Agraft, J. C. Cuevas, A. L. Yeyati, B. Ludoph, A. Martin-Rodero, G. R. Bollinger, J. M. van Ruitenbeek, and C. Urbina, Nature **394**, 154 (1998).
[13]J. M. Krans, J. M. van Ruitenbeek, V. V. Fisun, I. K. Yanson, and L. J. de Jongh, Nature **375**, 767 (1995).
[14]O. I. Shklyarevskii, and I. K. Yanson, Fiz. Nizk. Temp. **39**, 367 (2013) [Low Temp. Phys. **39**, 285 (2013)].
[15]J. A. Torres, J. I. Pascual, and J. J. Saenz, Phys. Rev. B **49**, 16581 (1994).
[16]J. A. Torres, and J. J. Saenz, Phys. Rev. Lett. **77**, 2245 (1996).
[17]A. G. M. Jansen, F. M. Mueller, and P. Wyder, Phys. Rev. B **16**, 1325 (1977).
[18]A. G. M. Jansen, F. M. Mueller, and P. Wyder, Science **199**, 1037 (1978).
[19]A. P. van Gelder, A. G. M. Jansen, and P. Wyder, Phys. Rev. B **22**, 1515 (1980).
[20]M. J. G. Lee, J. Caro, D. G. de Groot, and R. Griessen, Phys. Rev. B **31**, 8244 (1985).
[21]E. C. Svensson, B. N. Brockhouse, and J. M. Rowe, Phys. Rev. **155**, 619 (1967).
[22]S. G. Das, Phys. Rev. B **7**, 2238 (1973).
[23]F. Strigl, C. Espy, M. Buckle, E. Scheer, and T. Pietsch, Nat. Commun. **6**, 6172 (2015).
[24]M. Ring, D. Weber, P. Haiber, F. Pauly, P. Nielaba, and E. Scheer, Nano Lett. **20**, 5773 (2020).
[25]A. I. Akimenko, A. B. Verkin, N. M. Ponomarenko, and K. Yanson, Fiz. Nyzk. Temp. **8**, 260 (1982) [Sov. J. Low Temp. Phys. **8**, 130 (1982)].
[26]C. Schirm, M. Matt, F. Pauly, J. C. Cuevas, P. Nielaba, and E. Scheer, Nat. Nanotech. **8**, 645 (2013).
[27]M. Ring, F. Pauly, P. Nielaba, and E. Scheer, Simulating bistable current-induced switching of metallic atomic contacts by electron-vibration scattering, preprint (2023), arXiv:2303.03309 [cond-mat.mes-hall].
[28]N. Agrait, C. Untiedt, G. Rubio-Bollinger, and S. Vieira, Phys. Rev. Lett. **88**, 216803 (2002).
[29]J. Krans, J. van Ruitenbeek, and L. de Jongh, Physica B Condens. Matter **218**, 228 (1996).
[30]J. M. van Ruitenbeek, A. Alvarez, I. Pineyro, C. Grahmann, P. Joyez, M. H. Devoret, D. Esteve, and C. Urbina, Rev. Sci. Instrum. **67**, 108 (1996).